Spatiotemporal Dynamics of Online Motor Correction Processing Revealed by High-density Electroencephalography

Citation: Dipietro, Laura, Howard Poizner, and Hermano I. Krebs. "Spatiotemporal Dynamics of Online Motor Correction Processing Revealed by High-Density Electroencephalography." Journal of Cognitive Neuroscience (February 24, 2014): 1–15. © Massachusetts Institute of Technology

As Published: http://dx.doi.org/10.1162/jocn_a_00593

Publisher: MIT Press

Persistent URL: http://hdl.handle.net/1721.1/87584

Version: Final published version: final published article, as it appeared in a journal, conference proceedings, or other formally published context

Spatiotemporal Dynamics of Online Motor Correction Processing Revealed by High-density Electroencephalography

Laura Dipietro[1], Howard Poizner[2], and Hermano I. Krebs[1]

Abstract

■ The ability to control online motor corrections is key to dealing with unexpected changes arising in the environment with which we interact. How the CNS controls online motor corrections is poorly understood, but evidence has accumulated in favor of a submovement-based model in which apparently continuous movement is segmented into distinct submovements. Although most studies have focused on submovements' kinematic features, direct links with the underlying neural dynamics have not been extensively explored. This study sought to identify an electroencephalographic signature of submovements. We elicited kinematic submovements using a double-step displacement paradigm. Participants moved their wrist toward a target whose direction could shift mid-movement with a 50% probability. Movement kinematics and cortical activity were concurrently recorded with a low-friction robotic device and high-density electroencephalography. Analysis of spatiotemporal dynamics of brain activation and its correlation with movement kinematics showed that the production of each kinematic submovement was accompanied by (1) stereotyped topographic scalp maps and (2) frontoparietal ERPs time-locked to submovements. Positive ERP peaks from frontocentral areas contralateral to the moving wrist preceded kinematic submovement peaks by 220–250 msec and were followed by positive ERP peaks from contralateral parietal areas (140–250 msec latency, 0–80 msec before submovement peaks). Moreover, individual subject variability in the latency of frontoparietal ERP components following the target shift significantly predicted variability in the latency of the corrective submovement. Our results are in concordance with evidence for the intermittent nature of continuous movement and elucidate the timing and role of frontoparietal activations in the generation and control of corrective submovements. ■

INTRODUCTION

An important feature of the motor system is the ability to correct movements online during unfamiliar tasks or as unexpected changes in environmental conditions arise, for example, as a sudden target change occurs. To achieve this goal, the CNS must be able to continuously modify ongoing motor commands. Since Woodworth's seminal work (Woodworth, 1899), numerous studies have investigated behavioral aspects of movements that require adjustments because of differential requirements of speed and trajectories (Flash & Henis, 1991; Abend, Bizzi, & Morasso, 1982; Morasso, 1981; Soechting & Lacquaniti, 1981), differential accuracy requirements (Novak, Miller, & Houk, 2000, 2002; Miall, Weir, & Stein, 1993; Milner, 1992; Milner & Ijaz, 1990), and manipulation of sensory feedback (Doeringer & Hogan, 1998).

Brain imaging and cellular recording studies have been sparse compared with behavioral studies, but they have consistently shown that frontoparietal areas play a key role in controlling online motor corrections (Archambault, Ferrari-Toniolo, & Battaglia-Mayer, 2011; Archambault, Caminiti, & Battaglia-Mayer, 2009; Tunik, Houk, & Grafton, 2009; Diedrichsen, Hashambhoy, Rane, & Shadmehr, 2005; Desmurget et al., 1999, 2001; Krebs, Brashers-Krug, et al., 1998).

The neural mechanisms underlying online control of motor corrections have been the subject of considerable debate. Adjustments might rely on a continuous motor process (Hoffmann, 2011) that draws on a predictive forward model of control (Desmurget & Grafton, 2000; Wolpert & Ghahramani, 2000) or on a feedback-based control mechanism (Goodale, Pelisson, & Prablanc, 1986). Considerable evidence has accumulated in favor of a submovement-based model, in which movement corrections are controlled through distinct submovements or elementary units of movement that can be combined to achieve smooth behavior (Dipietro, Krebs, Fasoli, Volpe, & Hogan, 2009; Barringer, Barto, Fishbach, & Houk, 2008; Fishbach, Roy, Bastianen, Miller, & Houk, 2007; Wisleder & Dounskaia, 2007; Milner, 1992; Flash & Henis, 1991; Milner & Ijaz, 1990). Further support for this model has come from kinematic recordings from stroke patients, whose movement speed profiles display isolated peaks in early phases of motor recovery but become smoother as recovery progresses (Dipietro et al., 2009; Rohrer et al.,

[1]Massachusetts Institute of Technology, [2]University of California-San Diego

doi:10.1162/jocn_a_00593

2004; Krebs, Aisen, Volpe, & Hogan, 1999). Yet another line of results compatible with the submovement model comes from neurophysiological recordings in monkeys. Single-unit activity recorded in posterior parietal cortex (Archambault et al., 2009, 2011), dorsal premotor cortex (Archambault et al., 2011), and motor cortex (Archambault et al., 2011; Georgopoulos, Kalaska, Caminiti, & Massey, 1983) during corrective reaching movements is highly correlated with the individual trajectory components in which the complex movement can be decomposed. Finally, further evidence for the submovement model comes from analysis of EMG signals during fast reaching movements with corrections. D'Avella, Portone, and Lacquaniti (2011) found the error-correction of ongoing muscle synergies was not continuous but was intermittent, producing overlapping corrective submovements.

Although submovements are regarded as a peripheral manifestation of intermittent output from motor areas in the brain, a direct link has only been shown by a few studies. Tunik et al. (2009) recently showed that the fMRI BOLD signal in the putamen and in cerebellar regions correlated with the number of submovements in a reaching task, implying the involvement of these structures in making online decisions about the need for and the type of corrective submovements to invoke under conditions of uncertainty in the sensorimotor plant. They also showed that the BOLD signal from parietal, motor, and premotor cortices correlated with movement amplitude, further supporting findings that neural control of online updating extends to frontoparietal circuits (Archambault et al., 2009, 2011; Tunik et al., 2009; Diedrichsen et al., 2005; Desmurget et al., 1999, 2001; Krebs, Brashers-Krug, et al., 1998).

Although these studies have mainly been devoted to identifying brain areas that might subserve control of online motor corrections, a characterization of the underlying neural dynamics is lacking. Arguably this is because of the limited temporal resolution of traditional neuroimaging techniques such as fMRI (Eliassen et al., 2008). To elucidate such dynamics not only is key to further our understanding of neural control of movement but also is becoming increasingly important to design neurorehabilitation technology (Ifft, Lebedev, & Nicolelis, 2012; Ang et al., 2010), and to assess its therapeutic effects (Dipietro, Plank, Poizner, & Krebs, 2012; Swann et al., 2011).

In this work, we concurrently recorded high-density EEG signals and movement kinematics to elucidate the spatiotemoral dynamics of cortical activation underlying the control of online motor corrections. Specifically, we sought to find an EEG signature of submovements, which we elicited with a classical double-step target displacement paradigm (Flash & Henis, 1991; Georgopoulos et al., 1983) in which participants were asked to perform center-out movements toward a target whose location could suddenly change. Although a few recent studies have investigated related aspects of motor production, such as EEG correlates of motor planning in center-out movements (Naranjo et al., 2007) and ERPs elicited by evaluation of outcome and target errors (Krigolson, Holroyd, Van Gyn, & Heath, 2008; Krigolson & Holroyd, 2007), this study presents the first exploration of EEG correlates of submovements.

METHODS

Participants

Pointing movements of the wrist were studied in seven healthy, right-handed, young adults (age 18–25 years) with no reported history of neurological disorders. Experiments were approved by MIT Press's Committee on the Use of Humans as Experimental Subjects and by the University of California-San Diego Institutional Review Board. All participants gave informed written consent.

Experimental Task

The participant set-up was similar to the one described in Vaisman, Dipietro, and Krebs (in press). Briefly, participants were seated in front of a computer screen that was adjusted for optimal viewing for each participant and positioned approximately 60 cm from the participant. Participants held the handle of the wrist robot (which was parallel to the screen) in their right hand (Figure 1). Their upper arm and distal forearm were restrained by Velcro-strapped belts, and their forearm rested comfortably in the parasaggital plane on a custom-built sled so that only wrist movements were used for the motor task. The initial state of the arm was midway between pronation and supination. The screen displayed eight outer targets (diameter 2.5 cm) placed in a circle and a central

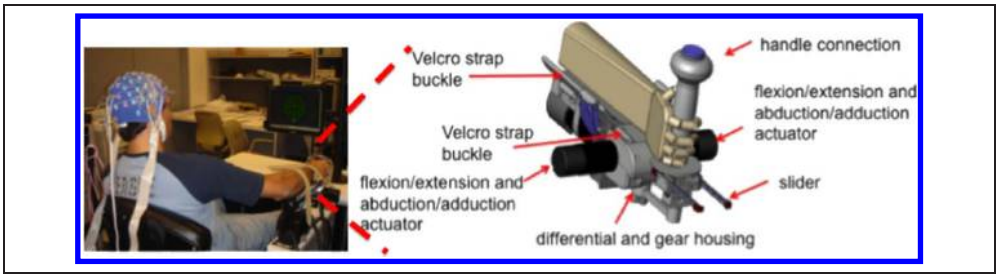

Figure 1. Experimental set-up (left) and wrist robot details (right).

target. Outer targets were presented in a pseudorandom order, and the central target was presented following presentation of an outer target. Participants were instructed to first move the handle of the robot to position the cursor in the central target and then move the handle of the robot to make the cursor reach one of the eight targets that was presented. The motor task required wrist flexion/extension and radial/ulnar deviation, which required 30° and 15° rotation, respectively. These selected ranges allowed for comfortable movements covering approximately 50% of the normal wrist range of motion (Vaisman et al., in press; Krebs et al., 2007). The amount of participants' wrist rotation was mapped to the position of a cursor that was shown on the screen.

The maximum time allotted for movement from the central target to an outer target or from the outer target to return to the central target was 1.4 sec. For the first 0.7 sec of this period, the target was one color and then turned to a different color. Participants were instructed to reach the target about when its color changed. The outer target might remain lit (control condition) or shift mid-movement to another outer target (shift condition). If the target changed location (shift condition), the participant was instructed to make a movement correction and move toward the new target location. The shift occurred at 0.4 sec after target onset with 50% probability. Participants performed 1280 wrist movements (640 movements from the central to the outer targets and 640 movements back), with 3-min rest breaks every 160 movements. Only movements from the central to the outer targets (i.e., 640 trials) were analyzed. Participants were allowed to practice until they were comfortable with the motor task.

An InMotion3 wrist robot (Interactive Motion Technologies, Watertown, MA) designed for clinical neurological applications was used in this study. The robot has three actuated degrees-of-freedom, namely radial/ulnar deviation, flexion–extension, and pronation–supination. A complete description of the hardware is reported elsewhere (Krebs et al., 2007). The angular positions of three encoders located at the joints of the robot were acquired digitally (sampling frequency f_s = 1000 Hz, 16-bit quantization). High-density scalp EEG was recorded continuously with a sampling rate of 1024 Hz, using 64 Ag/AgCl Active-Two electrodes placed in an elastic cap (Biosemi, Amsterdam, the Netherlands), corresponding to the International 10–10 system (Jasper, 1958), recorded relative to a DRL/CMS reference. The DRL/CMS electrodes were placed immediately lateral to POz; DRL was placed between POz and PO4, and CMS was placed between POz and PO3.

Kinematic Data Processing

Speed profiles of movements from the central to the outer targets were calculated as root square of the sum of squared velocity components. Velocity components were obtained from the first-time derivatives of position data smoothed with a low-pass 12-Hz zero-phase FIR filter. Gaussian-shaped submovements were extracted from the movement speed profiles using a greedy algorithm as described in Krebs, Hogan, Aisen, and Volpe (1998). Then, for each participant, submovements with the highest peak were selected from each movement trial (one submovement for the control and two submovements for the shift condition, one preshift and one postshift). Their parameters, namely latencies of peak value, of onset and offset (defined as the time when the submovement went respectively above and below 5% of its peak value), as well as peak value and sigma or standard deviation were calculated.

EEG Data Processing

EEG analysis was performed using the EEGLAB toolbox (Delorme & Makeig, 2004) for Matlab (MathWorks, Natick, MA). EEG data were first re-referenced to the average reference (Gwin & Ferris, 2012a, 2012b; Gwin, Gramann, Makeig, & Ferris, 2010). Then, they were high-pass filtered with a 1-Hz zero-phase FIR filter to remove offset and trend and downsampled to 128 Hz. Time intervals containing stereotypical artifacts, for example, excessive peak-to-peak deflections or bursts of EMG activity, were rejected by visual inspection and excluded from further analyses. Following removal of data sections containing artifacts identified via visual inspection, EEG data were further inspected for artifacts with a procedure based on independent component analysis (ICA) and dipole analysis, a standard method for removal of artifacts from EEG (Gwin & Ferris, 2012a, 2012b; Gwin et al., 2010; Hammon, Makeig, Poizner, Todorov, & de Sa, 2008; Delorme & Makeig, 2004; Makeig et al., 2002, 2004; Jung et al., 2000). For artifact rejection, we used InfoMax ICA (Jung et al., 2000; Bell & Sejnowski, 1995), which aims to minimize mutual information between sources by maximizing entropy. Independent components (ICs) were analyzed with respect to scalp topography and frequency characteristics, and those that displayed features indicative of artifacts were removed. The ICs were derived from the full set of trials (i.e., control and shift conditions), which is a standard procedure (Gwin et al., 2010). However, to the extent that artifact and brain components are not completely independent of one another and also are condition specific, removing artifacts from the combined data set might tend to cause a bias toward finding similar signals. This would be the case because removal of a given set of artifacts from the combined data set might theoretically also contain condition-specific brain components. Nonetheless, ICA finds the maximally ICs (although the independence may not be 100%), which would mitigate any such bias toward finding similarity. More importantly, though, subjecting the data to two different background artifact subtractions might cause spurious differences, which is likely to be more problematic. Eye movement artifacts were identified

according to the criteria described in the literature (Delorme & Makeig, 2004): EEG spectra were smoothly decreasing, a strong far-frontal projection was seen in the IC, and the IC's ERP image showed large voltage fluctuations corresponding to individual eye movements. Muscle artifacts were identified by ICs having a spatially focal scalp projection and high power at high frequencies (20–50 Hz and above). Dipole models were fit to the remaining components using the DIPFIT plug-in for EEGLAB and localized within a three-shell boundary element model of the Montreal Neurological Institute standard brain. Only the ICs whose dipoles resided within the brain volume of the head model and displayed less than 15% residual variance were retained. Cleaned EEG data were generated by projecting back the time course of activity within the remaining ICs to the surface electrodes. This procedure allows removal of artifacts from the EEG without having to reject the entire trial during which an artifact occurred (Jung et al., 2000).

EEG activity was then epoched 200 msec before and 1400 msec after the presentation of the outer target or visual stimulus, for which linear detrend and baseline correction procedures were applied. Epochs were then aligned and averaged, separately for each experimental condition (control or shift). ERPs were computed separately for each participant relative to the 200 msec prestimulus baseline. An average of 283 ± 26 and 294 ± 34 epochs per participant was retained for the control and shift condition respectively.

Statistical Analysis

Pearson's correlation coefficients were used to quantify similarities among ERP topographic scalp maps. Statistical significance was set at the .05 probability level, and a Bonferroni correction was applied for multiple comparisons ($p = .0036$). Two-tailed t tests (significance level = .05) were used to test for statistical differences between latencies of signal features derived from kinematic submovements and ERPs.

RESULTS

Movement Kinematics

Control Condition

Wrist speed profiles were similar across participants, demonstrating single peak/bell-shaped characteristics (see Figure 2, top). Speed profile decomposition typically returned a primary submovement, occasionally followed by small corrective submovements occurring close to the target (Milner & Ijaz, 1990). Our analysis focused on the primary submovement (see Methods). Average submovement onset, peak, and offset across participants occurred respectively at 250 ± 49 msec, 430 ± 57 msec, and 611 ± 66 msec after stimulus onset (target presentation); average submovement peak amplitude and sigma were respectively 1.7 ± 0.2 rad/sec and 73 ± 4 msec.

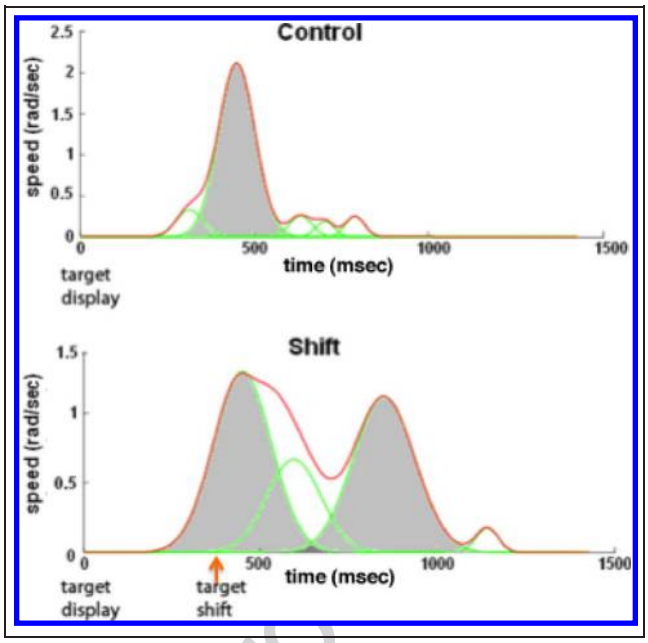

Figure 2. Examples of speed profiles (red) and decomposition into submovements (green) for the control (top) and shift (bottom) condition for Participant 1 (single trial). The main submovements are defined as the submovements with the highest peaks (highlighted in gray).

Shift Condition

Movements were initially directed toward the first target and then changed direction and moved to the second target. Speed profiles displayed two main peaks, which corresponded to the movement toward the first and second targets (see Figure 2, bottom). Speed profile decomposition returned two main submovements, one preshift and one postshift, which could be accompanied by smaller submovements positioned between them and/or at the end of the movement. Our analysis focused on the two main submovements (see Methods). Smaller submovements were removed because they were not present consistently across trials and to make kinematic data analysis consistent with EEG data analysis, which focused on averaged data (see below). For each participant, parameters of the first submovement (average onset, peak, and offset occurred respectively at 246 ± 40 msec, 424 ± 49 msec, and 602 ± 59 msec after stimulus onset; average amplitude and sigma were respectively 1.8 ± 0.2 rad/sec and 73 ± 5 msec) were very similar to the corresponding parameters of the submovement extracted from the control condition. The second submovement (average onset, peak, and offset occurred respectively at 713 ± 88 msec, 901 ± 95 msec, and 1086 ± 99 msec after stimulus onset; average amplitude and sigma were respectively 2.4 ± 0.2 rad/sec and 76 ± 3 msec)

was taller ($t(6) = -5.22$, $p < .01$) and wider (i.e., had a greater sigma; $t(6) = -2.55$, $p = .04$) than the first submovement.

ERP Topographic Scalp Maps and Relationship with Kinematic Data across Conditions

An average of 10.1 ± 3.3 ICs per participant were retained (average of 49.7 ± 3.0 ICs per participant excluded). Figure 3 presents typical examples of an IC that was removed (Figure 3, top) and retained (Figure 3, bottom).

Control Condition

The top panel of Figure 4 shows typical ERP topographic scalp maps. Consistently across participants, in the interval between target presentation at 0 and 200 msec, cortical activity was characterized by increased negativity over parietal-occipital areas that peaked at about 200 msec. This peak occurred just before the onset of the kinematic submovement, which occurred around 250 msec (average across participants). This timing of activation is consistent not only with the known role of the parieto-occipital cortex in target localization but also with the critical role of the posterior parietal cortex in online visuomotor control (Hauschild, Mulliken, Fineman, Loeb, & Andersen, 2012; Bernier, Burle, Hasbroucq, & Blouin, 2009; Baldauf, Cui, & Andersen, 2008; Desmurget et al., 1999).

At 300 msec, all participants also displayed similar cortical activations, which were characterized by a negative deflection in voltage over the frontal and central areas, including the sensorimotor areas. This timing of activation is consistent with findings showing that certain components of motor-related cortical potentials extend more than 100 msec after the onset of EMG activity, even for simple one-joint finger movements (Tarkka & Hallett,

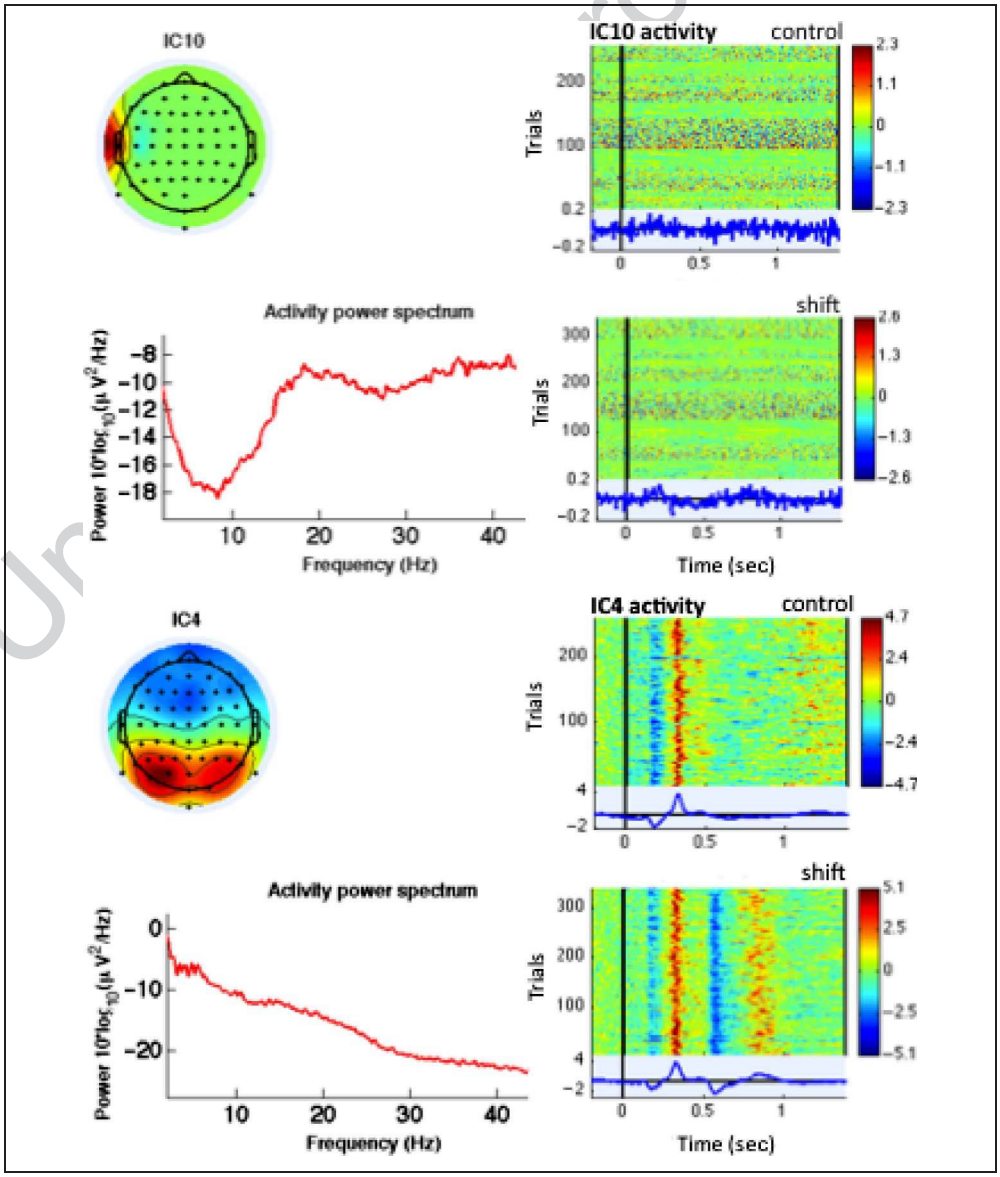

Figure 3. Examples of ICs from Participant 1. Scalp topographies, power spectra, and ERP images are shown. In the ERP images, the vertical black line indicates when the visual target was presented to the participant. IC10 displays a scalp topography having a focal point of activation located near the neck, a power spectrum with increasing power at high frequencies, and an ERP image in which there is constant activation for the full duration of a number of trials and little activation at all in the remaining trials. These patterns are indicative of muscle activity. In contrast, IC4 displays a scalp topography having activations located in the brain (and with a dipole-like structure), a power spectrum smoothly decreasing, and an ERP image showing variation in scalp potentials over the course of a trial. These patterns are indicative of brain activity.

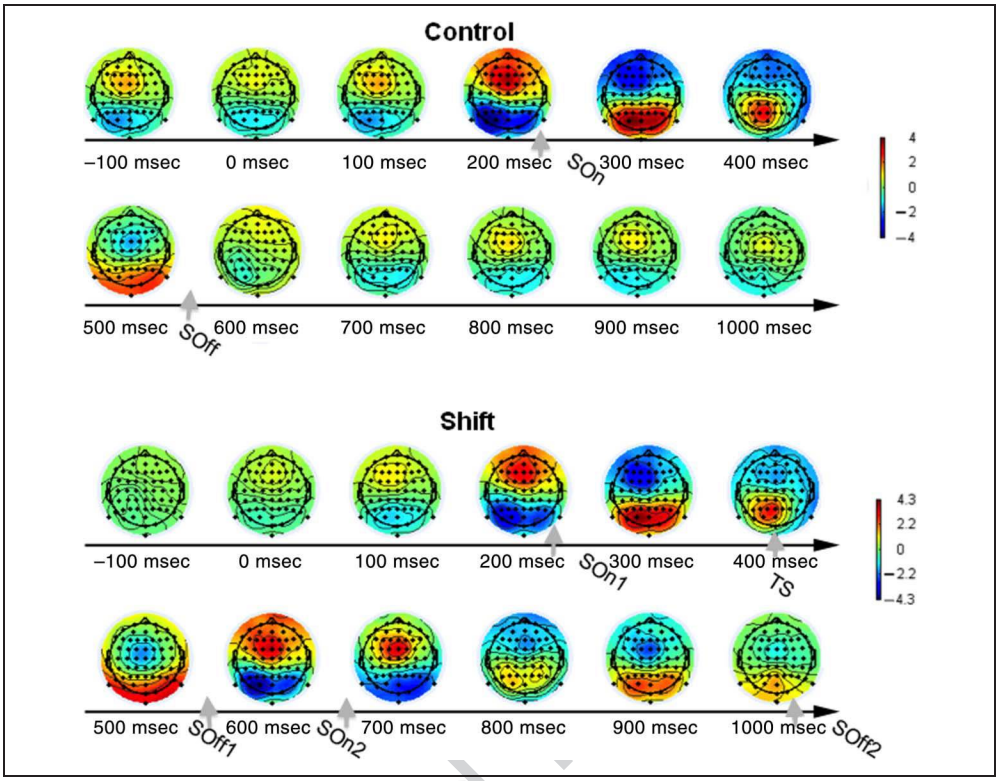

Figure 4. Topographic ERP scalp map series for Participant 1 for control (top) and shift (bottom) condition (100-msec interval). Target was presented at 0 msec. For the control condition, submovement onset/offset occurred at SOn/SOff; for the shift condition, target shift occurred at Ts; submovement onset/offset occurred at SOn1/SOff1 and SOn2/SOff2 for the preshift and postshift movement phase, respectively (see arrows). Note the similarity between maps for the two conditions at latencies 0–500 msec. Also note that in the shift condition maps at 600–1000 msec are similar to maps at 200–500 msec.

1991). Indeed, subdural recordings of supplementary motor cortex have shown negative potentials lasting up to 500 msec after movement onset (Neshige, Lüders, & Shibasaki, 1988). These potentials are likely because of somatosensory feedback from the movement (Tarkka & Hallett, 1991).

Shift Condition

The bottom panel of Figure 4 shows typical ERP topographic scalp maps. In the preshift phase of the shift condition, topographic maps were similar to the maps associated with the control condition, indicating a similar underlying cortical activation (compare bottom and top panels of Figure 4). Similarity was quantified by Pearson's correlations between topographic maps for the control and shift conditions, which ranged .85–.94 (average correlations were .85 ± .14 at 100 msec, .94 ± .10 at 200 msec, .93 ± .12 at 300 msec, and .90 ± .05 at 400 msec; correlations were highly significant for each participant). Within the first 200 msec from target presentation, all participants displayed similar scalp maps. As indicated by the correlation values reported in Table 1, scalp maps at 200 msec were similar to those at 0 and 100 msec. Similar to the control condition, cortical activity in this time interval was characterized by negative voltage deflections in electrode sites over the parietal-occipital region that peaked at about 200 msec. This peak occurred just before the onset of the first kinematic submovement (average submovement onset across participants was 246 msec) and was followed by a negative deflection in electrode sites over frontocentral sites, which peaked around 300 msec. After the target shift occurred, scalp maps that were observed before the target shift reoccurred. Specifically, the activation we observed at 200 msec reoccurred at 600–700 msec, depending on the participant, as indicated by the high and significant positive correlations between scalp maps (see Table 1). Similar to the preshift and control data, the peak amplitude of the negative deflection occurred before the second kinematic submovement onset (average submovement onset was 713 msec). The activation we observed at 300 msec also reoccurred at 800–1000 msec, depending on the participant, as indicated by the high and significant positive correlations (see Table 2). The temporal synchronization between ERP topographic scalp maps and submovement production (onset) suggests that neural activations associated with kinematic submovements are of stereotypical nature.

ERPs Recorded over Motor and Parietal Cortices and Relationship with Movement Kinematics

To further characterize the spatiotemoral dynamics of neural activation underlying our wrist pointing task, we analyzed trial-by-trial ERP activity associated with recordings over motor and parietal areas, which are known to be involved in control of online motor corrections (Archambault et al., 2011; Naranjo et al., 2007; Georgopoulos et al., 1983). For this purpose, we focused

Table 1. Correlation Analysis for ERP Topographic Scalp Maps in the Shift Condition (0.2 sec)

Time (sec)	*Sub #1*	*Sub #2*	*Sub #3*	*Sub #4*	*Sub #5*	*Sub #6*	*Sub #7*
0	.98*	.58*	.86*	.91*	.95*	−.30 (.01)	.87*
0.1	.95*	.87*	.71*	.87*	.98*	.31 (.01)	.83*
0.2	1*	1*	1*	1*	1*	1*	1*
0.3	−.95*	−.60*	−.78*	−.82*	−.81*	−.97*	−.80*
0.4	−.72*	−.67*	−.70*	−.66*	.02	−.89*	−.85*
0.5	−.65*	−.07	−.37*	−.35* .0069	−.91*	−.01	.45*
0.6	.97*	.28 (.02)	.11	.85*	−.09	.92*	.86*
0.7	.87*	−.03	.57*	.24 (.06)	.96*	.84*	.58*
0.8	−.89*	−.38*	.33 (.008)	.67*	.97*	−.27 (.03)	−.94*
0.9	−.91*	−.42*	−.15	−.75*	.84*	−.90*	−.73*
1.0	−.81*	.28	.44*	−.92*	−.93*	.15	−.39*
1.1	.94*	.19	−.78*	−.97*	−.89*	.05	−.24
1.2	.89*	.12	−.17	.03	−.59*	.33 (.008)	.26 (.04)
1.3	.76*	−.58*	.35 (.005)	.83*	.88*	.41*	.94*
1.4	.95*	−.39*	−.54*	.65*	.91*	.57*	.71*

Pearson's correlation coefficients between topographic scalp maps at 0.2 sec and topographic scalp maps at 0–1.4 sec, at 0.1-sec intervals, are reported. *p* Values are reported in brackets, and * indicates statistical significance ($p < .0036$). Topographic scalp maps displayed at 0.2 sec reappeared at 0.6–0.7 sec, as highlighted in gray.

Table 2. Correlation Analysis for ERP Topographic Scalp Maps in the Shift Condition (0.3 sec)

Time (sec)	*Sub #1*	*Sub #2*	*Sub #3*	*Sub #4*	*Sub #5*	*Sub #6*	*Sub #7*
0	−.95*	−.24	−.72*	−.65*	−.90*	.29 (.02)	−.96*
0.1	−.97*	−.88*	−.48*	−.75*	−.84*	−.35 (.005)	−.95*
0.2	−.95*	−.60*	−.78*	−.82*	−.81*	−.97*	−.80*
0.3	1*	1*	1*	1*	1*	1*	1*
0.4	.68*	.55*	.26 (.04)	.41*	.27 (.03)	.80*	.96*
0.5	.74*	−.66*	.35 (.004)	.35 (.006)	.58*	.07	−.10
0.6	−.96*	−.73*	.05	−.65*	−.24	−.95*	−.48*
0.7	−.91*	−.04	−.14	.05	−.91*	−.76*	−.87*
0.8	.83*	.92*	−.44*	−.55*	−.81*	.21	.91*
0.9	.96*	.95*	−.19	.61*	−.45*	.92*	.96*
1.0	.86*	−.009	−.48*	.80*	.94*	−.03	.85*
1.1	−.82*	−.81*	.63*	.85*	.90*	.01	.73*
1.2	−.77*	−.24	.63*	−.04	.10	−.23	.32 (.01)
1.3	−.79*	.05	.10	−.72*	−.96*	−.23	−.81*
1.4	−.94*	−.17	.64*	−.50*	−.93*	−.43*	−.94*

Pearson's correlation coefficients between topographic scalp maps at 0.3 sec and topographic scalp maps at 0–1.4 sec, at 0.1 sec intervals, are reported. *p* Values are reported in brackets, and * indicates statistical significance ($p \leq .0036$). Topographic scalp maps displayed at 0.3 sec reappeared at 0.8–1.3 sec, as highlighted in gray.

on recordings from C1 (contralateral motor cortex) and P1 (contralateral parietal cortex). Recordings from C3 and P3 displayed similar features.

Control Condition

The top panel of Figure 5 shows the trial-by-trial ERP activity as well as the grand average for electrode C1 for a typical participant. A slow negative potential shift was observed that increased in amplitude until target presentation. Here, a positive ERP component became predominantly active (a feature enhanced by our signal processing technique). This positive potential was observed consistently across participants at 213 ± 93 msec, preceding kinematic submovement peaks by 217 ± 62 msec, and was then followed by a negative potential. These data are consistent with previously published motor-related potentials that are known to accompany execution of voluntary movement (see, e.g., Tarkka & Hallett, 1991). The top panel of Figure 6 shows the trial-by-trial ERP activity as well as the grand average for electrode P1 for a typical participant. A positive potential peaking at 351 ± 47 msec was observed consistently across participants. This potential peaked on average 138 ± 106 msec later than the positive potential peaks observed at electrode C1 and 79 ± 87 msec before the submovement peak.

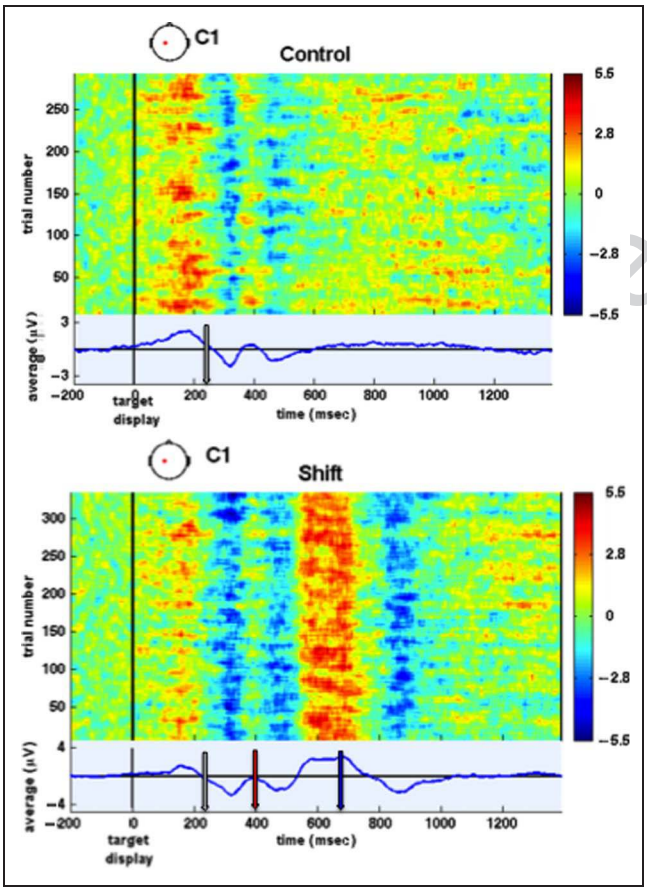

Figure 5. ERP image of channel C1 for the control (top) and shift (bottom) condition for Participant 1. Amplitude of EEG recordings during individual trials is shown. The vertical black line indicates when the visual target was presented to the participant. The red arrows indicates target shift. The gray and blue arrows indicate submovement onsets (average across the participant's trials). The ERP signal is shown as the blue trace at the bottom of each panel.

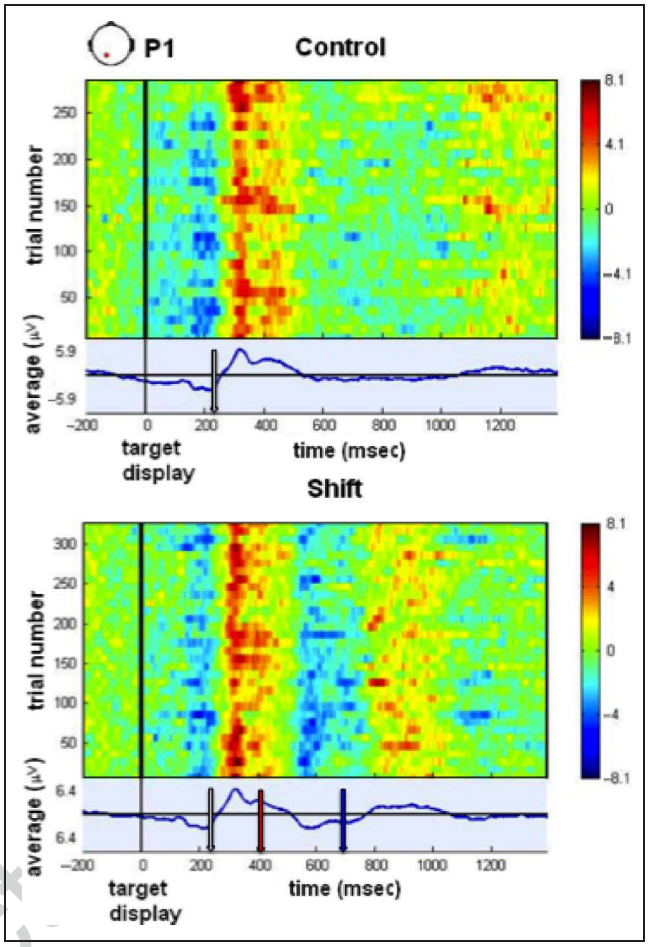

Figure 6. ERP image of channel P1 for the control (top) and shift (bottom) condition for Participant 1. Amplitude of EEG recordings during individual trials is shown. The vertical black line indicates when the visual target was presented to the participant. The red arrows indicates target shift. The gray and blue arrows indicate submovement onsets (average across the participant's trials). The ERP signal is shown as the blue trace at the bottom of each panel.

Shift Condition

The bottom panel of Figure 5 shows the trial-by-trial ERP activity as well as the grand average for electrode C1. The postshift phase of the shift condition displayed features similar to those displayed by the ERP images and signals across trials recorded in the control and preshift phase of the shift condition. This suggests that neural activity underlying the motor correction evoked by the target shift was similar to neural activity evoked by target presentation at 0 msec.

Positive potential peaks at electrode C1 were observed at 197 ± 97 msec and 654 ± 89 msec after target onset, that is, 226 ± 77 msec and 247 ± 56 msec before the first and second kinematic submovement peak, respectively. Statistical analysis showed no significant difference in the distances between C1 ERP-positive peaks and kinematic submovement peaks in the preshift, postshift, and control condition. This result indicates that the C1-positive potential peaks were time-locked to submovement peaks, leading them by approximately 220–250 msec.

The bottom panel of Figure 6 shows the trial-by-trial ERP activity as well as the grand average for electrode P1 for a typical participant. A positive potential, similar to the one observed for the control condition, was observed at 343 ± 39 msec after target onset. A second positive potential peaking at 900 ± 92 msec was also observed. ERP-positive potential peaks at electrode P1 were observed on average 146 ± 104 msec and 246 ± 52 msec after the positive peaks recorded at C1 in the pre- and postshift phase of movement, respectively (80 ± 70 msec and 0.7 ± 48 msec before the first and second submovement peak). Statistical analysis showed no statistical difference in the distances between ERP peaks at P1 and ERP peaks at C1 for the preshift, postshift, and control condition. Results were consistent across participants and suggest a sequential activation of motor and parietal areas. The timing of this sequential activation is consistent with the key role of the posterior parietal cortex in online visuomotor control (Hauschild et al., 2012; Bernier et al., 2009; Baldauf et al., 2008; Desmurget et al., 1999). The peak ERP activity over parieto-occipital cortex occurred well after peak activity over motor cortex and nearly simultaneously with the peak of the second submovement in the shift condition. The timing pattern also is generally consistent with Archambault et al. (2011), who recorded single unit activity in motor cortex and parietal cortex while monkeys reached to spatial targets that could shift location. Activations in motor cortex preceded those in parietal cortex, with peak parietal activations occurring during the movement correction in shift trials (Archambault et al., 2011).

While we focused our EEG analysis on ERP peaks latencies, we note that ERP shapes varied slightly across participants, especially after target shift at 600–700 msec. Such variability possibly reflects the kinematic variability observed in the behavioral data (e.g., extra submovements). Interestingly, individual participant variability in the latency of frontoparietal ERP components significantly predicted the variability in the after-shift submovement latency (correlation was .82, $p = .02$, for C1, and .87, $p = .01$, for P1); however, further analysis is warranted to fully characterize the relationship between kinematic and EEG variability, especially in this time window. Source localization may help elucidate ERP shape features and subcomponents' functional roles. For comparison purposes, we also analyzed trial-by-trial ERP activities at electrode C2 (ipsilateral motor cortex). ERPs at C2 displayed similar features to those recorded at C1 (see Figure 7), but their amplitudes were lower. This reduced amplitude is consistent with results from several previous studies that showed that ipsilateral and contralateral motor cortex operate in a similar fashion but with scaled levels of activation (Spraker, Yu, Corcos, & Vaillancourt, 2007; Dettmers et al., 1995).

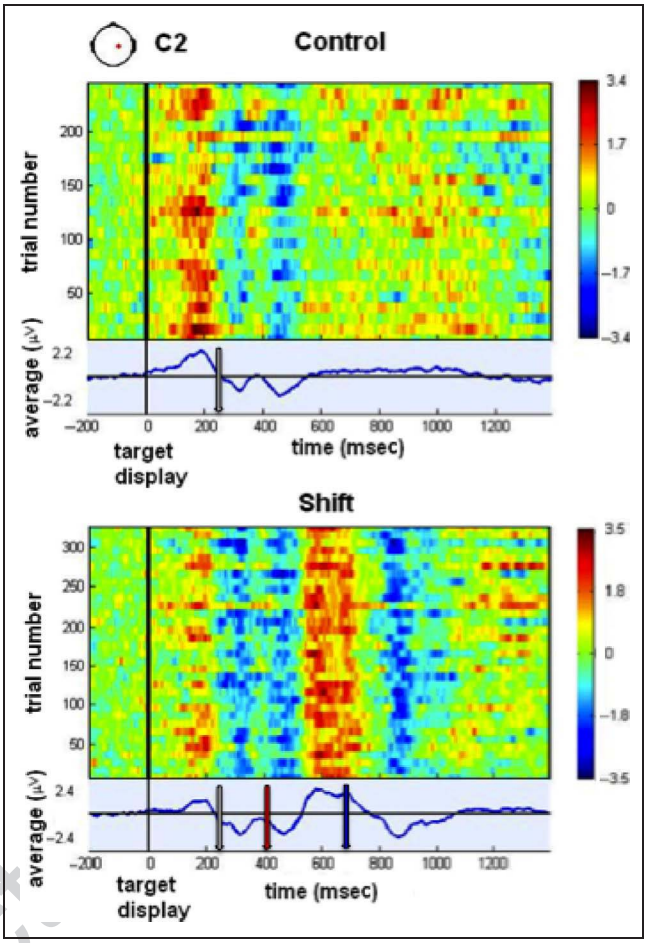

Figure 7. ERP image and signal of channel C2 for the control (top) and shift (bottom) condition for Participant 1. The vertical black line indicates when the visual target was presented to the participant. The red arrow indicates target shift. The gray and blue arrows indicate submovement onsets (average across the participant's trials). Compare with Figure 5: ERPs have shapes similar to corresponding ERPs recorded from channel C1 but lower amplitudes.

DISCUSSION

In this study, we sought to find an EEG signature of submovements. We found that ERP components in defined regions within a frontal-parieto-occipital network contralateral to the moving wrist exhibited intermittencies and that ERP intermittencies correlated with kinematic intermittencies. Specifically, we showed that the generation of each kinematic submovement was consistently accompanied by the occurrence of stereotyped ERP topographic

scalp maps and ERP components in defined regions within a frontal-parieto-occipital network contralateral to the moving wrist. In the control condition and in the preshift phase of the shift condition, the parietal-occipital and frontal-central activations occurred consistently in all participants with the generation of a new submovement. These activation patterns reoccurred after target shift, although with higher intersubject variability in duration and timing, especially in the frontal-central areas, which may well be because of submovement overlap (Henis & Flash, 1995). Although we simplified our analysis by reducing the kinematics to one (control) or two (shift) submovements, the actual kinematic patterns were more complex and presumably accompanied by more complex activations. Our results complement and extend the results of the preliminary studies on primates by Fishbach, Roy, Bastianen, Miller, and Houk (2003) and Roy et al. (2003). They analyzed the activity of neurons in the primary motor cortex and found it to be time-locked to just before the initiation of submovements.

EEG Signature of Online Corrective Submovements

How the CNS controls online motor commands to cope with environmental changes has been studied intensively for over three decades but remains only partially understood. Evidence has accumulated that such complex motor behavior is constructed by superimposing distinct submovements that have a stereotyped shape and whose features can be modulated based on motor task demands (Fishbach et al., 2007; Fishbach, Roy, Bastianen, Miller, & Houk, 2005; Novak et al., 2000, 2002; Krebs et al., 1999; Doeringer & Hogan, 1998; Henis & Flash, 1995; Miall et al., 1993; Milner, 1992; Flash & Henis, 1991; Milner & Ijaz, 1990; Morasso & Mussa Ivaldi, 1982; Woodworth, 1899).

The idea that the CNS generates and controls movement that we perceive as continuous and smooth in an intermittent fashion has been corroborated by a number of different studies. In the acute phase of motor recovery, movements performed by stroke patients are characterized by intermittent speed profiles, which can be modeled with isolated submovements that have a remarkably stereotyped shape and tend to progressively blend as recovery progresses (Dipietro et al., 2009; Rohrer et al., 2002; Krebs, Brashers-Krug, et al., 1998; Platz, Denzler, Kaden, & Mauritz, 1994). Specifically, the increases in movement smoothness that characterize both the acute and chronic phase of motor recovery from stroke can be explained by a submovement-based model, in which submovements become progressively longer, taller, fewer, and more overlapping (Dipietro et al., 2009; Rohrer et al., 2002). Vallbo and Wessberg (1993) showed that the kinematics of apparently continuous slow finger movements in fact displayed intermittencies that correlated with intermittencies in EMG. Gross et al. (2002) extended these results and found synchronization between pulsatile activity in a cerebello-thalamo-cortical loop and intermittencies in EMG activity.

Although previous studies have suggested that fronto-parietal areas are involved in the control of online motor corrections (Archambault et al., 2009, 2011; Tunik et al., 2009; Diedrichsen et al., 2005; Desmurget et al., 1999, 2001; Krebs, Brashers-Krug, et al., 1998) and possibly in the generation and control of underlying submovements (Tunik et al., 2009; Fishbach et al., 2003), the spatio-temporal dynamics of activation of these areas has not been studied in humans. EEG allows recordings of brain activations with resolution of the orders of milliseconds (Eliassen et al., 2008) and can thus elucidate the dynamics of cortical activation associated with such motor tasks.

Timing of Recordings over Motor and Parietal Cortices during Online Motor Corrections

It has been long known that motor-related cortical potentials (MRCP) accompany planning and execution of movements (Deecke, Scheid, & Kornhuber, 1969). Although the potentials associated with simple movements have been characterized in detail, how they are modulated as a result of a movement correction is unclear. Potentials associated with simple movement production, for example, movements to a single target, are known to have several subcomponents. These include the "Readiness Potential" or Bereitschaftspotentials (BP), that is, a negative potential that develops slowly and begins up to 1.5 sec before the initiation of a voluntary movement (Cui, Huter, Lang, & Deecke, 1999); the negative slope (NS), that is, a steeper increase in negativity; and the motor potential, that is, a further increase in negativity that appears around movement onset and peaks shortly after (Wiese et al., 2005; Tarkka & Hallett, 1991). Although their exact functional role is still unclear (Fabiani, Gratton, & Federmeier, 2007), these different MRCP subcomponents are thought to represent activity of specific cortical areas responsible for movement planning and execution. For example, the early BP is thought to represent predominantly SMA activity, the NS probably reflects both SMA and contralateral motor cortex activity, and later components of the MRCP likely reflect sensorimotor and other cortical activation (Jankelowitz & Colebatch, 2002, 2005). Consistent with such findings, brain lesions are known to have a differential effect on MRCP subcomponents depending on the lesion site (Wiese, Stude, Nebel, Osenberg, Ischebeck, et al., 2004; Wiese, Stude, Nebel, Osenberg, Volzke, et al., 2004; Gerloff, 2003). Alterations of MRCPs have been reported in a number of studies on participants recovering from stroke (Wiese et al., 2005; Platz et al., 2000; Green, Bialy, Sora, & Ricamato, 1999; Kopp et al., 1999; Honda et al., 1997; Kitamura, Shibasaki, & Takeuchi, 1996), and alterations of BPs have been specifically observed in patients with traumatic brain injury (Di Russo, Incoccia, Formisano, Sabatini, & Zoccolotti, 2005), Parkinson's disease and

cerebellar ataxia (Shibasaki, Shima, & Kuroiwa, 1978), and lesions in the SMA (Deecke, Lang, Heller, Hufnagl, & Kornhuber, 1987).

ERPs recorded in our control condition (single target movements) at electrode C1 (located over left motor cortex), which were similar to those recorded at the same electrode in the preshift phase of the shift condition, displayed a very small BP wave. This was probably because of the relatively short movement preparation time and externally cued movement. The BP was followed by a high positive peak (enhanced by the signal processing technique) and by a negative motor potential wave. Although to the best of our knowledge MRCPs associated with online movement corrections have not been characterized, our recordings show that they are composed of two neural complexes that display similar features. Although further analysis is warranted to elucidate the exact location of their sources, the similarity displayed by neural and kinematic features we observed between the pre- and postshift suggests that the second complex may have an origin similar to the first complex and thus partially reflect activation of SMA and contralateral M1 areas. Timing of these complexes also suggests that they reflect not only motor-related but also somatosensory-related activation, consistent with findings that so somatosensory- and motor-related activations typically are inseparably intertwined (Petreanu et al., 2012; Flanders, 2011; Ostry, Darainy, Mattar, Wong, & Gribble, 2010; Kleinfeld, Ahissar, & Diamond, 2006). Motor cortex cells respond to somatosensory stimulation (Evarts & Fromm, 1977), somatosensory cortex can directly activate movement even with motor cortex inactivated (Matyas et al., 2010), loss of proprioception produces marked deficits in motor control (Sainburg, Ghilardi, Poizner, & Ghez, 1995; Sainburg, Poizner, & Ghez, 1993), efference copies of motor commands represent expected sensory states during movements (Flanders, 2011), and sensory and motor plasticity are linked (Ostry et al., 2010; Nasir & Ostry, 2009).

ERPs recorded at electrode P1, located over left posterior parietal cortex, in the control and shift condition argue for a role of the posterior parietal cortex in reach planning and adjustment of reaching online, consistent with previous results (Battaglia-Mayer et al., 2012; Hauschild et al., 2012; Archambault et al., 2009, 2011; Desmurget et al., 1999). Moreover, the timing of P1 peaks relative to C1 peaks is consistent with that reported by Bernier et al. (2009) for single reaches to visual targets. ERPs recorded at electrode P1 in the preshift phase of the shift condition in this study were similar to those recorded at the same electrode in the control condition. However, we observed a greater (although not statistically significant, $t(6) = -1.99$, $p = .09$, delay between the positive peaks recorded at P1 and C1 in the postshift phase of the shift condition compared with the preshift phase. This greater delay may reflect the increased demand placed on parietal cortices in creating an internal model of the changed environment and the associated changes in the state of the limb, both of which are necessary for updating the initial movement path (Archambault et al., 2011; Krigolson et al., 2008). EEG recordings have extremely good temporal resolution but do not provide precise spatial localization, because they necessarily capture very large populations of cells. Because voltage fields fall off with the square of distance from the source, it is generally true that underlying cortices near the recording electrode produce the strongest signal; however, this is by no means always true (Fize, Fabre-Thorpe, Richard, Doyon, & Thorpe, 2005). These qualifications should be borne in mind in interpreting the above-mentioned ERP findings.

Brain Networks Underlying Online Motor Corrections

Although investigations of neural mechanisms governing error detection and recalibration of visuomotor tracking and online control of reaching and grasping have identified a distributed network encompassing BG, cerebellum, frontal, and parietal areas (Tunik, Schmitt, & Grafton, 2007; Krakauer et al., 2004; Desmurget et al., 2001; Ghilardi et al., 2000), the neural circuits subserving submovement generation and control remain relatively unexplored. However, the roles of the motor cortex and posterior parietal cortex in mediating online movement corrections have been clearly demonstrated. Early work by Georgopoulos et al. (1983) showed that in nonhuman primates the firing activity of M1 neurons was interrupted by a target shift and replaced by the pattern of M1 activity related to the movement toward the new target. More recently, Fishbach et al. (2003) found M1 activity in monkeys was time-locked to just before the initiation of submovements.

The posterior parietal cortex contains viewer-centered spatial maps important for reaching movements and plays a key role in visual action planning (Lindner, Iyer, Kagan, & Andersen, 2010). There is a tight relationship between parietal cell activity and hand kinematics when monkeys must correct an ongoing reaching movement for a shift in target location (Archambault et al., 2009). This modulation of parietal cell activity often leads and thus predicts the change in movement trajectory in response to the target shift (Archambault et al., 2009). Moreover, temporarily inactivating the anterior intraparietal sulcus via TMS creates significant delays in online adjustments of grasp (Tunik, Frey, & Grafton, 2005). Consistent with the role of posterior parietal cortex in planning upcoming movements, patients with lesions in the posterior parietal cortex fail to adjust their ongoing movements to shifts in target location (Grea et al., 2002) and show not only spatial impairments but also impaired reach timing and smoothness (Torres, Raymer, Gonzalez Rothi, Heilman, & Poizner, 2010). Our results both confirm and extend these findings.

The interplay between parietal and motor cortical areas in online movement corrections is only beginning

to be examined. Recently, Archambault et al. (2011) recorded cell activity in premotor dorsal and primary motor cortex whereas monkeys reached to targets that suddenly shifted spatial location during the movement and compared these activations to those in posterior parietal cortex. Archambault et al. (2011) found that all three regions simultaneously encoded the initial movement plan (reaching in one direction) and an updated plan (reaching in a different direction following the target shift), but with different timing relative to movement trajectory changes. The order of activation of these areas was premotor dorsal, primary motor, and, finally, posterior parietal cortex. We found a similar sequential evolution of ERP activity from recordings over motor cortical regions to recordings over posterior parietal cortex in relation to submovement peaks.

Conclusions

We used high-density EEG recordings to investigate the dynamics of cortical activation underlying online motor corrections. We used a classical double-step target displacement protocol to evoke kinematic submovements and recorded underlying brain activity with high-density EEG. We found that production of kinematic submovements was accompanied by stereotyped ERP topographic scalp maps. Moreover, peaks of ERP components recorded over motor cortical and parietal areas were time-locked to kinematic submovement peaks. Our findings are consistent with a growing body of evidence for the intermittent nature of continuous movement and for a submovement-based model of control of online motor corrections (but do not constitute unequivocal proof for them). They also elucidate the temporal evolution of neural signals associated with submovements and, specifically, the temporal relationships between posterior and central activations in mediating submovements.

UNCITED REFERENCE

Desmurget et al., 2004

Acknowledgments

We thank Markus Plank for his helpful comments on the manuscript and Klaus Gramman for his help with EEGLAB. This study was supported in part by NIH R01-HD045343, NIH R01-NS036449, ONR MURI Award N000140811114, NSF Grant SMA-1041755 to the Temporal Dynamics of Learning Center and NSF Science of Learning Center, and ENG-1137279 (EFRI M3C). H. I. Krebs is a coinventor in several MIT-held patents for the robotic technology. He holds equity positions in Interactive Motion Technologies, Watertown, MA, USA, the company that manufactures robotic technology under license to MIT Press.

Reprint requests should be sent to Laura Dipietro, Department of Mechanical Engineering, Massachusetts Institute of Technology, 77 Massachusetts Avenue 3-147, Cambridge, MA 02139, or via e-mail: lauradp@mit.edu.

REFERENCES

Abend, W., Bizzi, E., & Morasso, P. (1982). Human arm trajectory formation. *Brain, 105,* 331–348.

Ang, K. K., Guan, C., Chua, K. S., Ang, B. T., Kuah, C., Wang, C., et al. (2010). Clinical study of neurorehabilitation in stroke using EEG-based motor imagery brain-computer interface with robotic feedback. *IEEE Engineering in Medicine and Biology Society, 2010,* 5549–5552.

Archambault, P. S., Caminiti, R., & Battaglia-Mayer, A. (2009). Cortical mechanisms for online control of hand movement trajectory: The role of the posterior parietal cortex. *Cerebral Cortex, 19,* 2848–2864.

Archambault, P. S., Ferrari-Toniolo, S., & Battaglia-Mayer, A. (2011). Online control of hand trajectory and evolution of motor intention in the parietofrontal system. *Journal of Neuroscience, 31,* 742–752.

Baldauf, D., Cui, H., & Andersen, R. A. (2008). The posterior parietal cortex encodes in parallel both goals for double-reach sequences. *Journal of Neuroscience, 28,* 10081–10089.

Barringer, C. W., Barto, A. G., Fishbach, A., & Houk, J. C. (2008). *Simulated reaching supports discrete control hypothesis for error-correction in voluntary limb movements*. Washington, DC: Society for Neuroscience.

Battaglia-Mayer, A., Ferrari-Toniolo, S., Visco-Comandini, F., Archambault, P. S., Saberi-Moghadam, S., & Caminiti, R. (2012). Impairment of online control of hand and eye movements in a monkey model of optic ataxia. *Cerebral Cortex*.

Bell, A. J., & Sejnowski, T. J. (1995). An information-maximization approach to blind separation and blind deconvolution. *Neural Computation, 7,* 1129–1159.

Bernier, P. M., Burle, B., Hasbroucq, T., & Blouin, J. (2009). Spatio-temporal dynamics of reach-related neural activity for visual and somatosensory targets. *Neuroimage, 47,* 1767–1777.

Cui, R. Q., Huter, D., Lang, W., & Deecke, L. (1999). Neuroimage of voluntary movement: Topography of the BP, a 64-ch DC current source density study. *Neuroimage, 9,* 124–134.

D'Avella, A., Portone, A., & Lacquaniti, F. (2011). Superposition and modulation of muscle synergies for reaching in response to a change in target location. *Journal of Neurophysiology, 106,* 2796–2812.

Deecke, L., Lang, W., Heller, H. J., Hufnagl, M., & Kornhuber, H. H. (1987). Bereitschaftspotential in patients with unilateral lesions of the supplementary motor area. *Journal of Neurology, Neurosurgery, and Psychiatry, 50,* 1430–1434.

Deecke, L., Scheid, P., & Kornhuber, H. H. (1969). Distribution of readiness potential, pre-motion positivity, and motor potential of the human cerebral cortex preceding voluntary finger movements. *Experimental Brain Research, 7,* 158–168.

Delorme, A., & Makeig, S. (2004). EEGLAB: An open source toolbox for analysis of single-trial EEG dynamics including ICA. *Journal of Neuroscience Methods, 134,* 9–21.

Desmurget, M., Epstein, C. M., Turner, R. S., Prablanc, C., Alexander, G. E., & Grafton, S. T. (1999). Role of the posterior parietal cortex in updating reaching movements to a visual target. *Nature Neuroscience, 2,* 563–567.

Desmurget, M., Gaveau, V., Vindras, P., Turner, R. S., Broussolle, E., & Thobois, S. (2004). On-line motor control in patients with Parkinson's disease. *Brain, 127,* 1755–1773.

Desmurget, M., & Grafton, S. (2000). Forward modeling allows feedback control for fast reaching movements. *Trends in Cognitive Sciences, 4,* 423–431.

Desmurget, M., Grea, H., Grethe, J. S., Prablanc, C., Alexander, G. E., & Grafton, S. T. (2001). Functional anatomy of nonvisual feedback loops during reaching: A PET study. *Journal of Neuroscience, 21,* 2919–2928.
Dettmers, C., Fink, G. R., Lemon, R. N., Stephan, K. M., Passingham, R. E., Silbersweig, D., et al. (1995). Relation between cerebral activity and force in the motor areas of the human brain. *Journal of Neurophysiology, 74,* 802–815.
Di Russo, F., Incoccia, C., Formisano, R., Sabatini, U., & Zoccolotti, P. (2005). Abnormal motor preparation in severe traumatic brain injury with good recovery. *Journal of Neurotrauma, 22,* 297–312.
Diedrichsen, J., Hashambhoy, Y., Rane, T., & Shadmehr, R. (2005). Neural correlates of reach errors. *Journal of Neuroscience, 25,* 9919–9931.
Dipietro, L., Krebs, H. I., Fasoli, S. E., Volpe, B. T., & Hogan, N. (2009). Submovement changes characterize generalization of motor recovery after stroke. *Cortex, 45,* 318–324.
Dipietro, L., Plank, M., Poizner, H., & Krebs, H. I. (2012). EEG microstate analysis in human motor corrections. In *Conference Proceedings on Biomedical Robotics and Biomechatronics*, Rome, Italy.
Doeringer, J. A., & Hogan, N. (1998). Intermittency in preplanned elbow movements persists in the absence of visual feedback. *Journal of Neurophysiology, 80,* 1787–1799.
Eliassen, J. C., Boespflug, E. L., Lamy, M., Allendorfer, J., Chu, W. J., & Szaflarski, J. P. (2008). Brain-mapping techniques for evaluating poststroke recovery and rehabilitation: A review. *Topics in Stroke Rehabilitation, 15,* 427–450.
Evarts, E. V., & Fromm, C. (1977). Sensory responses in motor cortex neurons during precise motor control. *Neuroscience Letters, 5,* 267–272.
Fabiani, M., Gratton, G., & Federmeier, K. D. (2007). Event-related brain potentials: Methods, theory and applications. In *Handbook of psychophysiology*. Cambridge University Press.
Fishbach, A., Roy, S. A., Bastianen, C., Miller, L. E., & Houk, J. C. (2003). *Neural correlates of on-line error correction in M1 of behaving macaque monkeys*. Society for NCM.
Fishbach, A., Roy, S. A., Bastianen, C., Miller, L. E., & Houk, J. C. (2005). Kinematic properties of on-line error corrections in the monkey. *Experimental Brain Research, 164,* 442–457.
Fishbach, A., Roy, S. A., Bastianen, C., Miller, L. E., & Houk, J. C. (2007). Deciding when and how to correct a movement: Discrete submovements as a decision making process. *Experimental Brain Research, 177,* 45–63.
Fize, D., Fabre-Thorpe, M., Richard, G., Doyon, B., & Thorpe, S. J. (2005). Rapid categorization of foveal and extrafoveal natural images: Associated ERPs and effects of lateralization. *Brain and Cognition, 59,* 145–158.
Flanders, M. (2011). What is the biological basis of sensorimotor integration? *Biological Cybernetics, 104,* 1–8.
Flash, T., & Henis, E. (1991). Arm trajectory modification during reaching towards visual targets. *Journal of Cognitive Neuroscience, 3,* 220–230.
Georgopoulos, A. P., Kalaska, J. F., Caminiti, R., & Massey, J. T. (1983). Interruption of motor cortical discharge subserving aimed arm movements. *Experimental Brain Research, 49,* 327–340.
Gerloff, C. (2003). Movement-related cortical potentials (MRCP) in patients with focal brain lesions. In *The Bereitschaftspotential. MRCP*. New York: Kluwer Academic/Plenum.
Ghilardi, M., Ghez, C., Dhawan, V., Moeller, J., Mentis, M., Nakamura, T., et al. (2000). Patterns of regional brain activation associated with different forms of motor learning. *Brain Research, 871,* 127–145.
Goodale, M. A., Pelisson, D., & Prablanc, C. (1986). Large adjustments in visually guided reaching do not depend on vision of the hand or perception of target displacement. *Nature, 320,* 748–750.
Grea, H., Pisella, L., Rossetti, Y., Desmurget, M., Tilikete, C., Grafton, S., et al. (2002). A lesion of the posterior parietal cortex disrupts on-line adjustments during aiming movements. *Neuropsychologia, 40,* 2471–2480.
Green, J. B., Bialy, Y., Sora, E., & Ricamato, A. (1999). High-resolution EEG in poststroke hemiparesis can identify ipsilateral generators during motor tasks. *Stroke, 30,* 2659–2665.
Gross, J., Timmermann, L., Kujala, J., Dirks, M., Schmitz, F., Salmelin, R., et al. (2002). The neural basis of intermittent motor control in humans. *Proceedings of the National Academy of Sciences, U.S.A., 99,* 2299–2302.
Gwin, J. T., & Ferris, D. P. (2012a). Beta- and gamma-range human lower limb corticomuscular coherence. *Frontiers in Human Neuroscience, 6,* 258.
Gwin, J. T., & Ferris, D. P. (2012b). An EEG-based study of discrete isometric and isotonic human lower limb muscle contractions. *Journal of Neuroengineering and Rehabilitation, 9,* 9–35.
Gwin, J. T., Gramann, K., Makeig, S., & Ferris, D. (2010). Removal of movement artifact from high-density EEG recorded during walking and running. *Journal of Neurophysiology, 103,* 3526–3534.
Hammon, P. S., Makeig, S., Poizner, H., Todorov, E., & de Sa, V. R. (2008). Predicting reaching targets from human EEG. *IEEE Signal Processing, 25,* 69–77.
Hauschild, M., Mulliken, G. H., Fineman, I., Loeb, G. E., & Andersen, R. A. (2012). Cognitive signals for brain-machine interfaces in posterior parietal cortex include continuous 3D trajectory commands. *Proceedings of the National Academy of Sciences, U.S.A., 109,* 17075–17080.
Henis, E. A., & Flash, T. (1995). Mechanisms underlying the generation of averaged modified trajectories. *Biological Cybernetics, 72,* 407–419.
Hoffmann, H. (2011). Target switching in curved human arm movements is predicted by changing a single control parameter. *Experimental Brain Research, 208,* 73–87.
Honda, M., Nagamine, T., Fukuyama, H., Yonekura, Y., Kimura, J., & Shibasaki, H. (1997). Movement-related cortical potentials and regional cerebral blood flow change in patients with stroke after motor recovery. *Journal of the Neurological Science, 146,* 117–126.
Ifft, P. J., Lebedev, M. A., & Nicolelis, M. A. (2012). Reprogramming movements: Extraction of motor intentions from cortical ensemble activity when movement goals change. *Frontiers in Neuroengineering, 5,* 16.
Jankelowitz, S. K., & Colebatch, J. G. (2002). Movement-related potentials associated with self-paced, cued and imagined arm movements. *Experimental Brain Research, 147,* 98–107.
Jankelowitz, S. K., & Colebatch, J. G. (2005). Movement related potentials in acutely induced weakness and stroke. *Experimental Brain Research, 161,* 104–113.
Jasper, H. H. (1958). The ten-twenty electrode system of the International Federation. *Electroencephalography and Clinical Neurophysiology, 10,* 371–375.
Jung, T. P., Makeig, S., Westerfield, M., Townsend, J., Courchesne, E., & Sejnowski, T. J. (2000). Removal of eye activity artifacts from visual event-related potentials in normal and clinical subjects. *Clinical Neurophysiology, 111,* 1745–1758.

Kitamura, J., Shibasaki, H., & Takeuchi, T. (1996). Cortical potentials preceding voluntary elbow movement in recovered hemiparesis. *Electroencephalography and Clinical Neurophysiology, 98,* 149–156.
Kleinfeld, D., Ahissar, E., & Diamond, M. E. (2006). Active sensation: Insights from the rodent vibrissa sensorimotor system. *Current Opinion in Neurobiology, 16,* 435–444.
Kopp, B., Kunkel, A., Muhlnickel, W., Villringer, K., Taub, E., & Flor, H. (1999). Plasticity in the motor system related to therapy-induced improvement of movement after stroke. *NeuroReport, 10,* 807–810.
Krakauer, J. W., Ghilardi, M. F., Mentis, M., Barnes, A., Veytsman, M., Eidelberg, D., et al. (2004). Differential cortical and subcortical activations in learning rotations and gains for reaching: A PET study. *Journal of Neurophysiology, 91,* 924–933.
Krebs, H. I., Aisen, M. L., Volpe, B. T., & Hogan, N. (1999). Quantization of continuous arm movements in humans with brain injury. *Proceedings of the National Academy of Sciences, U.S.A., 96,* 4645–4649.
Krebs, H. I., Brashers-Krug, T., Rauch, S. L., Savage, C. R., Hogan, N., Rubin, R. H., et al. (1998). Robot-aided functional imaging: Application to a motor learning study. *Human Brain Mapping, 6,* 59–72.
Krebs, H. I., Hogan, N., Aisen, M. L., & Volpe, B. T. (1998). Robot-aided neurorehabilitation. *IEEE Transactions on Neural Systems and Rehabilitation Engineering, 6,* 75–87.
Krebs, H. I., Volpe, B. T., Williams, D., Celestino, J., Charles, S. K., Lynch, D., et al. (2007). Robot-aided neurorehabilitation: A robot for wrist rehabilitation. *IEEE Transactions on Neural Systems and Rehabilitation Engineering, 15,* 327–335.
Krigolson, O. E., & Holroyd, C. B. (2007). Hierarchical error processing: Different errors, different systems. *Brain Research, 1155,* 70–80.
Krigolson, O. E., Holroyd, C. B., Van Gyn, G., & Heath, M. (2008). Electroencephalographic correlates of target and outcome errors. *Experimental Brain Research, 190,* 401–411.
Lindner, A., Iyer, A., Kagan, I., & Andersen, R. A. (2010). Human posterior parietal cortex plans where to reach and what to avoid. *Journal of Neuroscience, 30,* 11715–11725.
Makeig, S., Delorme, A., Westerfield, M., Jung, T. P., Townsend, J., Courchesne, E., et al. (2004). Electroencephalographic brain dynamics following manually responded visual targets. *PLoS Biology, 2,* e176.
Makeig, S., Westerfield, M., Jung, T. P., Enghoff, S., Townsend, J., Courchesne, E., et al. (2002). Dynamic brain sources of visual evoked responses. *Science, 295,* 690–694.
Matyas, F., Sreenivasan, V., Marbach, F., Wacongne, C., Barsy, B., Mateo, C., et al. (2010). Motor control by sensory cortex. *Science, 330,* 1240–1243.
Miall, R. C., Weir, D. J., & Stein, J. F. (1993). Intermittency in human manual tracking tasks. *Journal of Motor Behavior, 25,* 53–63.
Milner, T. E. (1992). A model for the generation of movements requiring endpoint precision. *Neuroscience, 49,* 487–496.
Milner, T. E., & Ijaz, M. M. (1990). The effect of accuracy constraints on three-dimensional movement kinematics. *Neuroscience, 35,* 365–374.
Morasso, P. (1981). Spatial control of arm movements. *Experimental Brain Research, 42,* 223–227.
Morasso, P., & Mussa Ivaldi, F. A. (1982). Trajectory formation and handwriting: A computational model. *Biological Cybernetics, 45,* 131–142.
Naranjo, J. R., Brovelli, A., Longo, R., Budai, R., Kristeva, R., & Battaglini, P. P. (2007). EEG dynamics of the frontoparietal network during reaching preparation in humans. *Neuroimage, 34,* 1673–1682.
Nasir, S. M., & Ostry, D. J. (2009). Auditory plasticity and speech motor learning. *Proceedings of the National Academy of Sciences, U.S.A., 106,* 20470–20475.
Neshige, R., Lüders, H., & Shibasaki, H. (1988). Recording of movement-related potentials from scalp and cortex in man. *Brain, 111,* 719–736.
Novak, K. E., Miller, L. E., & Houk, J. C. (2000). Kinematic properties of rapid hand movements in a knob turning task. *Experimental Brain Research, 132,* 419–433.
Novak, K. E., Miller, L. E., & Houk, J. C. (2002). The use of overlapping submovements in the control of rapid hand movements. *Experimental Brain Research, 144,* 351–364.
Ostry, D. J., Darainy, M., Mattar, A. A., Wong, J., & Gribble, P. L. (2010). Somatosensory plasticity and motor learning. *Journal of Neuroscience, 30,* 5384–5393.
Petreanu, L., Gutnisky, D. A., Huber, D., Xu, N. L., O'Connor, D. H., Tian, L., et al. (2012). Activity in motor-sensory projections reveals distributed coding in somatosensation. *Nature, 489,* 299–303.
Platz, T., Denzler, P., Kaden, B., & Mauritz, K. H. (1994). Motor learning after recovery from hemiparesis. *Neuropsychologia, 32,* 1209–1223.
Platz, T., Kim, I. H., Pintschovius, H., Winter, T., Kieselbach, A., Villringer, K., et al. (2000). Multimodal EEG analysis in man suggests impairment-specific changes in movement-related electric brain activity after stroke. *Brain, 123,* 2475–2490.
Rohrer, B., Fasoli, S., Krebs, H. I., Hughes, R., Volpe, B., Frontera, W., et al. (2002). Movement smoothness changes during stroke recovery. *Journal of Neuroscience, 22,* 8297–8304.
Rohrer, B., Fasoli, S., Krebs, H. I., Volpe, B., Frontera, W. R., Stein, J., et al. (2004). Submovements grow larger, fewer, and more blended during stroke recovery. *Motor Control, 8,* 472–483.
Roy, S. A., Bastianen, C., Nenonene, E., Fishbach, A., Miller, L. E., & Houk, J. C. (2003). *Neural correlates of corrective submovement formation in the basal ganglia and motor cortex*. Society for NCM.
Sainburg, R. L., Ghilardi, M. F., Poizner, H., & Ghez, C. (1995). Control of limb dynamics in normal subjects and patients without proprioception. *Journal of Neurophysiology, 73,* 820–835.
Sainburg, R. L., Poizner, H., & Ghez, C. (1993). Loss of proprioception produces deficits in interjoint coordination. *Journal of Neurophysiology, 70,* 2136–2147.
Shibasaki, H., Shima, F., & Kuroiwa, Y. (1978). Clinical studies of the movement-related cortical potential (MP) and the relationship between the dentatorubrothalamic pathway and readiness potential (RP). *Journal of Neurology, 219,* 15–25.
Soechting, J. F., & Lacquaniti, F. (1981). Invariant characteristics of a pointing movement in man. *Journal of Neuroscience, 1,* 710–720.
Spraker, M. B., Yu, H., Corcos, D. M., & Vaillancourt, D. E. (2007). Role of individual basal ganglia nuclei in force amplitude generation. *Journal of Neurophysiology, 98,* 821–834.
Swann, N., Poizner, H., Houser, M., Gould, S., Greenhouse, I., Cai, W., et al. (2011). DBS of the subthalamic nucleus alters the cortical profile of response inhibition in the beta frequency band: A scalp EEG study in PD. *Journal of Neuroscience, 31,* 5721–5729.
Tarkka, I. M., & Hallett, M. (1991). Topography of scalp-recorded motor potentials in human finger movements. *Journal of Clinical Neurophysiology, 8,* 331–341.

Torres, E. B., Raymer, A., Gonzalez Rothi, L. J., Heilman, K. M., & Poizner, H. (2010). Sensory-spatial transformations in the left posterior parietal cortex may contribute to reach timing. *Journal of Neurophysiology, 104,* 2375–2388.

Tunik, E., Frey, S. H., & Grafton, S. T. (2005). Virtual lesions of the anterior intraparietal area disrupt goal-dependent on-line adjustments of grasp. *Nature Neuroscience, 8,* 505–511.

Tunik, E., Houk, J. C., & Grafton, S. T. (2009). Basal ganglia contribution to the initiation of corrective submovements. *Neuroimage, 47,* 1757–1766.

Tunik, E., Schmitt, P. J., & Grafton, S. T. (2007). BOLD coherence reveals segregated functional neural interactions when adapting to distinct torque perturbations. *Journal of Neurophysiology, 97,* 2107–2120.

Vaisman, L., Dipietro, L., & Krebs, H. I. (in press). A comparative analysis of speed profile models for wrist pointing movements. *IEEE Transactions on Neural Systems and Rehabilitation Engineering*.

Vallbo, A. B., & Wessberg, J. (1993). Organization of motor output in slow finger movements in man. *Journal of Physiology, 469,* 673–691.

Wiese, H., Stude, P., Nebel, K., Osenberg, D., Ischebeck, W., Stolke, D., et al. (2004). Recovery of movement-related potentials in the temporal course after prefrontal traumatic brain injury: A follow-up study. *Clinical Neurophysiology, 115,* 2677–2692.

Wiese, H., Stude, P., Nebel, K., Osenberg, D., Volzke, V., Ischebeck, W., et al. (2004). Impaired movement-related potentials in acute frontal traumatic brain injury. *Clinical Neurophysiology, 115,* 289–298.

Wiese, H., Stude, P., Sarge, R., Nebel, K., Diener, H. C., & Keidel, M. (2005). Reorganization of motor execution rather than preparation in poststroke hemiparesis. *Stroke, 36,* 1474–1479.

Wisleder, D., & Dounskaia, N. (2007). The role of different submovement types during pointing to a target. *Experimental Brain Research, 176,* 132–149.

Wolpert, D. M., & Ghahramani, Z. (2000). Computational principles of movement neuroscience. *Nature Neuroscience, 3(Suppl.),* 1212–1217.

Woodworth, R. S. (1899). The accuracy of voluntary movements. *Psychological Review, 3,* 1–114.